

## Supporting Information:

### Charge Transport in a Two-Dimensional Hybrid Metal Halide Thiocyanate Compound

John G. Labram,<sup>a,†</sup> Naveen R. Venkatesan,<sup>a,†</sup> Christopher J. Takacs,<sup>a</sup> Hayden A. Evans,<sup>a,b,c</sup> Erin E. Perry,<sup>a</sup> Fred Wudl,<sup>a,b,c</sup> Michael L. Chabinyc<sup>a,b,\*</sup>

---

<sup>a.</sup> *Department of Materials and Mitsubishi Chemical Center for Advanced Materials, University of California Santa Barbara, Santa Barbara, CA, 93106, USA.*

<sup>b.</sup> *Materials Research Laboratory, University of California Santa Barbara, Santa Barbara, CA, 93106, USA*

<sup>c.</sup> *Department of Chemistry and Biochemistry, University of California Santa Barbara, Santa Barbara, CA, 93106, USA*

<sup>†.</sup> These authors contributed equally to this work.

<sup>\*</sup> Email: mchabinyc@engineering.ucsb.edu

### S1 Evaluation of Time-Resolved Microwave Conductivity Figure of Merit

A diagrammatic representation of the time-resolved microwave conductivity (TRMC) system employed in this study is shown in Figure 6 of the main text.

The microwave detectors employed in our system output a voltage that is linearly proportional to the incident microwave power  $P$ . The photo-induced change in sample conductance  $\Delta G$ , is related to the normalized change in microwave power ( $\Delta P/P$ ) via Equation (S1):<sup>1-3</sup>

$$\Delta G(t) = -\frac{1}{K} \frac{\Delta P(t)}{P} \quad (\text{S1})$$

Since  $\Delta G$  is dependent on the normalized change in microwave power  $\Delta P/P$ , it is not necessary to know the absolute values of microwave power, just the relative change under illumination. For this reason, with a knowledge of the detector voltage in the dark  $V$ , and the change under illumination  $\Delta V$ , it is possible to determine the photo-induced conductance from the signal voltage:

$$\Delta G(t) = -\frac{1}{K} \frac{\Delta V(t)}{V} \quad (\text{S2})$$

Here,  $K$  is the sensitivity factor of the cavity. Assuming the electric field in the cavity possesses an integer number of half-wavelengths (as is the case for TE/TEM modes) this parameter can be derived<sup>4</sup> for a cavity filled with a conducting medium to be:

$$K^{(full)} = -\frac{\left(1 + \frac{1}{\sqrt{R_0}}\right)Q}{\pi f_0 \epsilon_0 \epsilon_r L \beta} \quad (\text{S3})$$

The parameters in Equation S3 are as follows:  $R_0$  is the reflectivity of the cavity to microwaves at the resonance frequency  $f_0$ .  $\epsilon_0$  and  $\epsilon_r$  are the vacuum permittivity and the relative permittivity of the medium of the cavity, respectively.  $L$  is the length of the cavity.  $\beta$  is the ratio of the two remaining cavity dimensions, with the numerator / denominator depending on the polarization direction of the standing wave. In our case  $\beta = 2.25$ .  $Q$  is the cavity quality factor, expressed as the ratio of the resonance frequency  $f_0$ , to the full-width at half-maximum  $\Delta W$ :

$$Q = \frac{f_0}{\Delta W} \quad (\text{S4})$$

To account for the fact we are studying the change in conductance of a thin film of thickness  $d$ , rather than a homogeneous medium filling the length of the cavity  $L$ , we multiply  $K^{(full)}$  by a correction factor  $g(L, d)$ , to account for the difference in integrated electric field magnitude over the region of interest:

$$K = g(L, d)K^{(full)} \quad (S5)$$

Where:

$$g(L, d) = \frac{\int_{z_0}^{z_0+d} \sin\left(\frac{\pi mz}{L}\right) dz}{\int_0^L \sin\left(\frac{\pi mz}{L}\right) dz} \quad (S6)$$

Here  $z_0$  is the position in the cavity where the sample is located and  $m$  is the integer number of half wavelengths of the electric field component in the cavity (which depends on the mode of the cavity). The sample position  $z_0$  is chosen to be at a maxima of the magnitude of the electric field, hence:  $z_0 = L[n + 1]/(2m)$  where  $n \in \mathbb{Z}$ . In the regime where  $L \ll d$ , as is the case in our experiment, the correction factor becomes the following for all  $m \in \mathbb{Z}$ :

$$g(L, d) = \frac{2d}{L} \quad (S7)$$

Therefore, for our thin-film TRMC experiment we use the following value of  $K$ :

$$K = -\frac{2Q\left(1 + \frac{1}{\sqrt{R_0}}\right)}{\pi f_0 \varepsilon_0 \varepsilon_r L \beta} \quad (S8)$$

Since our measurements are carried out in air, and the sample thickness is typically  $\sim 100$  nm –  $1 \mu\text{m}$ , we have here approximated  $\varepsilon_r = 1$ . The relative permittivity of  $\text{CH}_3\text{NH}_3\text{PbI}_3$  is known<sup>5</sup> to be  $\sim 10$ . However, since the film is only  $\sim 100$  nm to  $\sim 1 \mu\text{m}$  thick and length of the cavity is  $\sim 100$  mm (i.e.  $10^5$  to  $10^6$  times longer), the weighted average in the cavity can to a very good approximation be assumed to be unity. To determine  $R_0$ ,  $f_0$  and  $\Delta W$  (and hence  $Q$ ), the reflectivity of the cavity must be evaluated as a function of microwave frequency. To achieve this, we make use of the reference channel on our TRMC design (see Figure 6 main text). Microwaves directed through the reference channel do not enter the cavity and hence the ratio of the signal to the reference signals provides the reflectivity of the cavity. **Figure S1** shows an example of the reflectivity of our loaded cavity as a function of microwave frequency, with approximate parameters extracted.

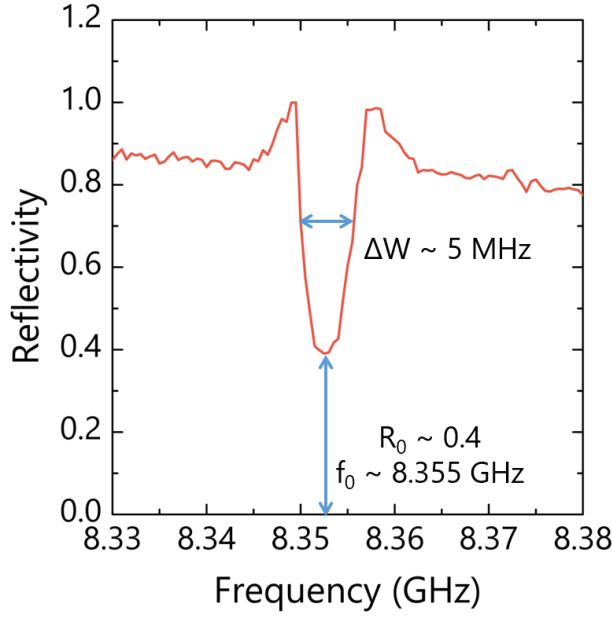


**Figure S1.** Frequency response of loaded microwave cavity, showing the detected reflectivity of the cavity as a function of incident frequency. The parameters  $f_0$ ,  $R_0$  and  $\Delta W$  can all be extracted from this plot as shown.

With the conductance  $\Delta G$  determined, The TRMC figure of merit can then be evaluated using the below relationship:<sup>2</sup>

$$\phi \Sigma \mu(t) = \frac{\Delta G(t)}{\beta e I_0 F_A M} \quad (\text{S9})$$

Here  $I_0$  is the fluence of laser (photons / unit area / pulse),  $e$  is the magnitude of the fundamental unit of charge, and  $F_A$  ( $\in [0,1]$ ) is the fraction of photons absorbed in the sample at the excitation wavelength. The parameter  $F_A$  was extracted from the optical transmittance spectra from Figure 2 main text to be 0.41 for  $\text{CH}_3\text{NH}_3\text{PbI}_3$  and 0.54 for  $(\text{CH}_3\text{NH}_3)_2\text{Pb}(\text{SCN})_2\text{I}_2$ . The parameter  $M$  ( $\in [0,1]$ ) is the fractional area of the sample in the cavity exposed to incident light; here evaluated via image analysis to be 0.101.

## S2. Purity of $(\text{CH}_3\text{NH}_3)_2\text{Pb}(\text{SCN})_2\text{I}_2$ films

**Figure S2** shows the experimental XRD spectra of films of  $(\text{CH}_3\text{NH}_3)_2\text{Pb}(\text{SCN})_2\text{I}_2$ , with calculated powder patterns of isotropic  $\text{CH}_3\text{NH}_3\text{PbI}_3$  and (100) aligned  $(\text{CH}_3\text{NH}_3)_2\text{Pb}(\text{SCN})_2\text{I}_2$ . Comparison of calculated spectra with measured spectra indicates no peaks from  $\text{CH}_3\text{NH}_3\text{PbI}_3$  in the thiocyanate-based film. Films of  $\text{CH}_3\text{NH}_3\text{PbI}_3$  are typically textured with a preferential orientation of the (110) direction; to account for the possibility of impurity domains in the thiocyanate film being randomly oriented with respect to the bulk, the isotropic powder pattern was used. The two peaks labelled with asterisks in the pattern of  $(\text{CH}_3\text{NH}_3)_2\text{Pb}(\text{SCN})_2\text{I}_2$  represent peaks that are unaccounted for. The unaccounted peak at approximately 7 degrees represents diffraction from a larger  $d$ -spacing than the  $(\text{CH}_3\text{NH}_3)_2\text{Pb}(\text{SCN})_2\text{I}_2$  layer spacing. These peaks neither belong to  $\text{CH}_3\text{NH}_3\text{PbI}_3$ , nor  $\text{PbI}_2$ . Because they appear at such a low

concentration, we believe that this unknown low concentration impurity should not appreciably affect our TRMC measurements.

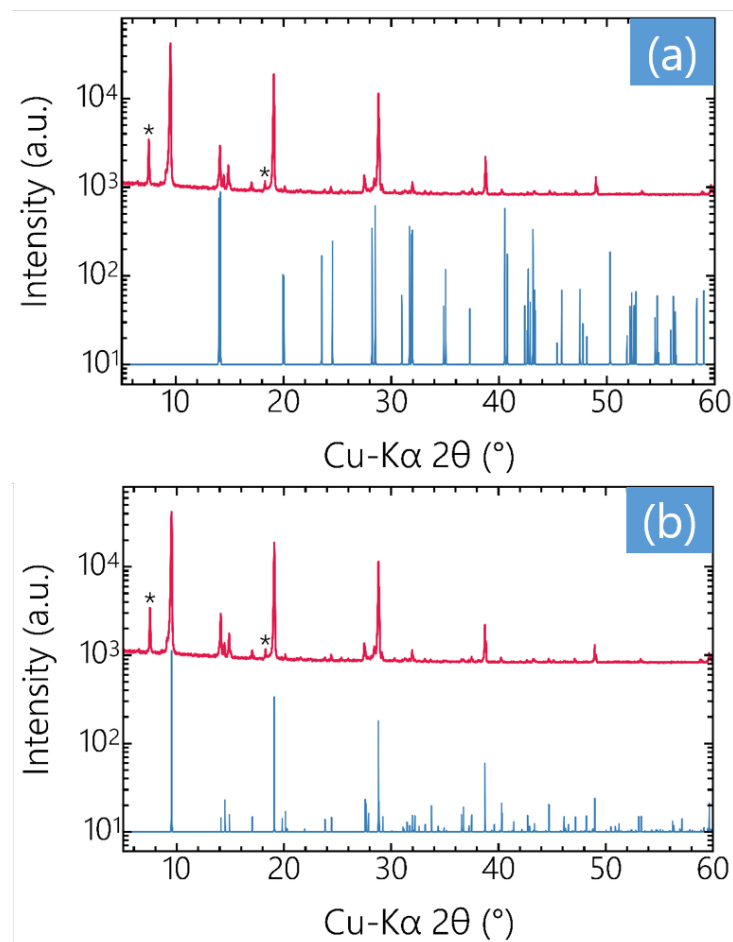


**Figure S2.** X-ray diffraction spectra of thin films of  $(\text{CH}_3\text{NH}_3)_2\text{Pb}(\text{SCN})_2\text{I}_2$  (red) plotted against calculated spectra (blue) of (a)  $\text{CH}_3\text{NH}_3\text{PbI}_3$  and (b) (100) oriented  $(\text{CH}_3\text{NH}_3)_2\text{Pb}(\text{SCN})_2\text{I}_2$  (planes parallel to the substrate), plotted on a logarithmic y-axis scale. Spectra were calculated as described in the Experimental Section of the main text.

### S3. Analysis of TRMC Decay Constants

The lifetime  $\tau$ , of carriers is determined by a number of processes (monomolecular, bimolecular and Auger),<sup>6</sup> that have different relative contributions at different carrier concentrations. For this reason, unambiguously extracting a single decay parameter from TRMC transients is challenging.<sup>7</sup> As illustrated by Figure 4(c) in the main text, the form of the decay is often complicated, and the time-dependence of the figure of merit cannot accurately be quantified by a small number of parameters. An approach previously taken to roughly quantify the decay is to fit a double exponential function and evaluate  $\tau$  as a weighted average of these constants.<sup>7</sup> To make comparison with the literature as easy as possible, we have here analyzed our data using a similar (but not identical) approach.

We have fitted the experimental data to a single exponential decay, in two separate regions of each plot - roughly defined as the fast and slow regions. These decay rates are labeled here  $\tau_1$

and  $\tau_2$ , with y-axis intercepts of  $C_1$  and  $C_2$  respectively. The representative decay constant  $\tau$ , is expressed as a weighted average of the two decays:

$$\tau = \frac{C_1\tau_1 + C_2\tau_2}{C_1 + C_2} \quad (\text{S10})$$

We have in this case not fitted directly to a double exponential function to avoid using 4 fitting parameters simultaneously per fit. **Figure S3** shows example TRMC traces for  $\text{CH}_3\text{NH}_3\text{PbI}_3$  and  $(\text{CH}_3\text{NH}_3)_2\text{Pb}(\text{SCN})_2\text{I}_2$  plotted with logarithmic y-axis scales, fitted to exponential functions in 2 regions of the plot. The values of  $\tau$  plotted in Figure 5(b) of the main text are evaluated using the weighted average of the two from Equation S10. As shown in Figure 4(c) of the main text and in Figure S3 below, the  $(\text{CH}_3\text{NH}_3)_2\text{Pb}(\text{SCN})_2\text{I}_2$  compound exhibits a very long-lived decay which cannot be accurately fitted using the techniques described here. For this reason, and to avoid ambiguity, values at lower fluence have not been included in the data in Figure 3(e) of the main text.

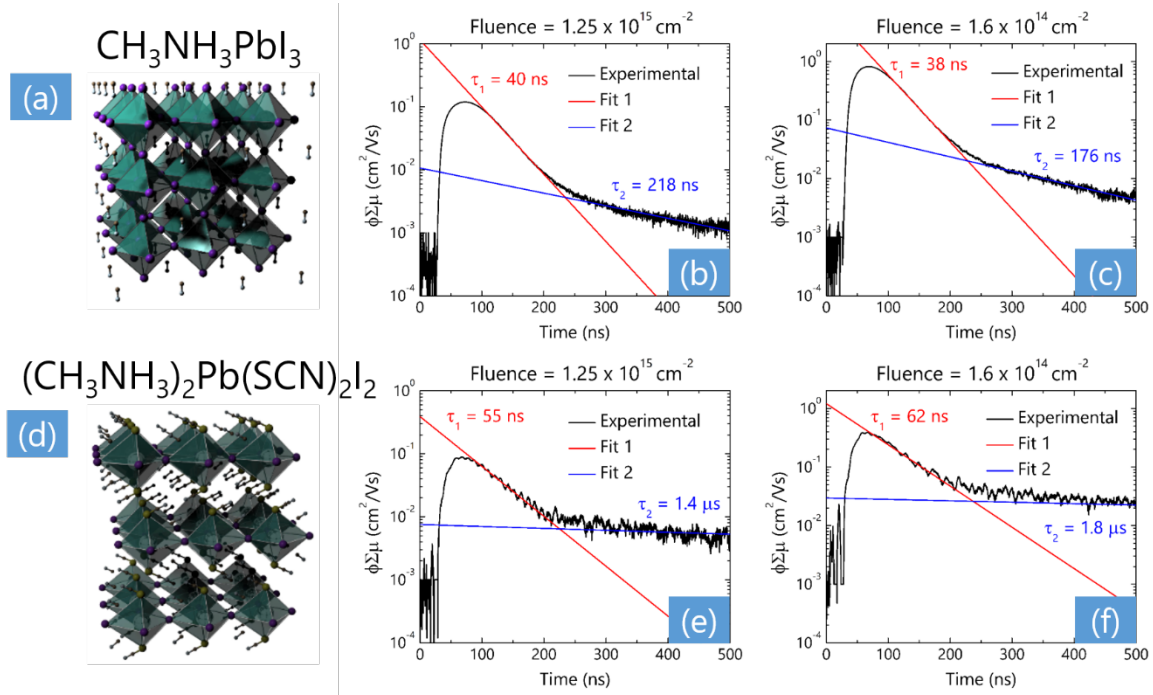


**Figure S3.** (a) Structure of methylammonium lead iodide ( $\text{CH}_3\text{NH}_3\text{PbI}_3$ ). Time-resolved microwave conductivity data (TRMC) plot ( $\phi\Sigma\mu$  as a function of time) of  $\text{CH}_3\text{NH}_3\text{PbI}_3$  plotted on a logarithmic scale at a (b) high and (c) low fluence. (d) Structure of Methylammonium Lead Thiocyanate Iodide ( $(\text{CH}_3\text{NH}_3)_2\text{Pb}(\text{SCN})_2\text{I}_2$ ). Time-resolved microwave conductivity data (TRMC) plot ( $\phi\Sigma\mu$  as a function of time) of  $(\text{CH}_3\text{NH}_3)_2\text{Pb}(\text{SCN})_2\text{I}_2$  plotted on a logarithmic scale at a (e) high and (f) low fluence.

#### S4. Verification of TRMC Figures of Merit

We conducted a set of repeated measurements to ensure that our extracted figure of merit ( $\phi\Sigma\mu$ ) is reliable and reproducible. **Figure S4** shows the extracted maximum figure of merit ( $\phi\Sigma\mu_{max}$ ) for films of (a)  $\text{CH}_3\text{NH}_3\text{PbI}_3$  and (b)  $(\text{CH}_3\text{NH}_3)_2\text{Pb}(\text{SCN})_2\text{I}_2$  as a function of incident fluence from Figure 5(a) of the main text combined with a repeated set of measurements for a different

film, prepared under identical conditions, on a different day. The data show broadly consistent values, indicative of a reliable and consistent measurement technique. The slight variations at low fluence are due to subjective ambiguity in extracting values of  $\phi\Sigma\mu_{max}$  from data with a low signal/noise ratio.

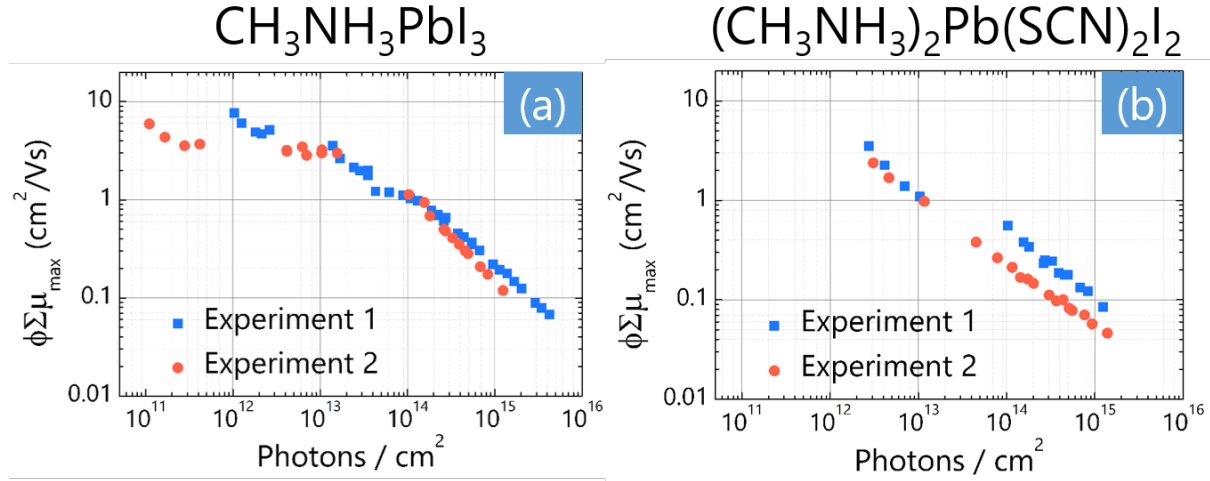


**Figure S4.** Extracted maximum time-resolved microwave conductivity (TRMC) figure of merit ( $\phi\Sigma\mu$ ) as a function of incident optical fluence for two films of (a)  $\text{CH}_3\text{NH}_3\text{PbI}_3$  and (b)  $(\text{CH}_3\text{NH}_3)_2\text{Pb}(\text{SCN})_2\text{I}_2$ , prepared and measured on different days.

To compare with previously measured values, **Figure S5** shows the same data plotted with values extracted from a recent publication by Oga *et. al.*<sup>3</sup>

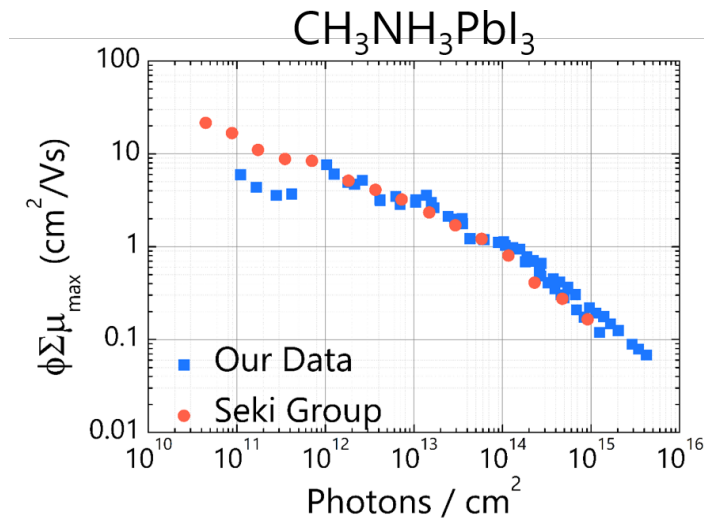


**Figure S5.** Extracted values of  $\phi\Sigma\mu_{max}$  as a function of incident optical fluence from both sets of data in Figure S4(a) plotted with previously reported values by the Seki group.<sup>3</sup>

### S5. Photoluminescence

Photoluminescence measurements of  $\text{CH}_3\text{NH}_3\text{PbI}_3$  and  $(\text{CH}_3\text{NH}_3)_2\text{Pb}(\text{SCN})_2\text{I}_2$  were carried out as described in the main text. Absorbance and emission spectra as a function of wavelength and energy are shown for both compounds in **Figure S6**. In both cases, the excitation wavelength used was 450 nm. Both materials appear to emit at very similar energies, however the purity of

the thiocyanate compound is confirmed by x-ray diffraction (Figure S2). The large Stokes shift seen in the  $(\text{CH}_3\text{NH}_3)_2\text{Pb}(\text{SCN})_2\text{I}_2$  optical data has recently been attributed to long-lived triplet states,<sup>8</sup> and may reconcile the long lifetimes seen in the TRMC data.

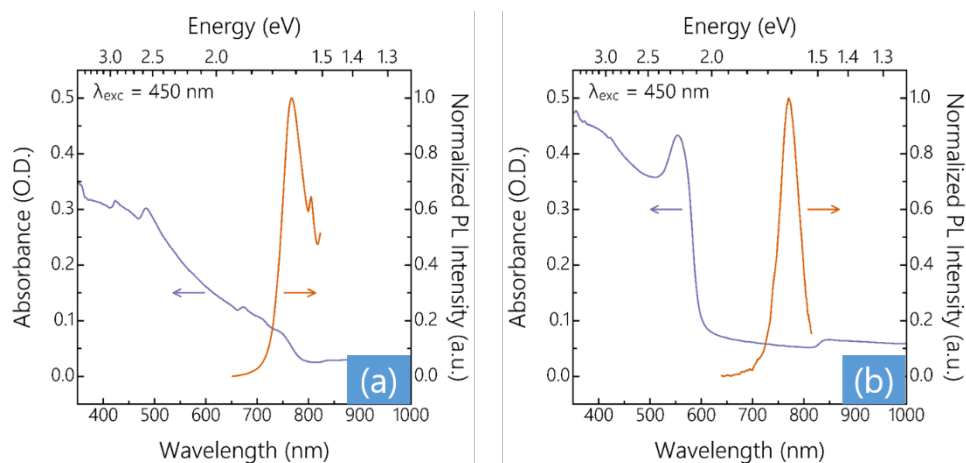


**Figure S6.** Absorbance and emission spectra of (a)  $\text{CH}_3\text{NH}_3\text{PbI}_3$  and (b)  $(\text{CH}_3\text{NH}_3)_2\text{Pb}(\text{SCN})_2\text{I}_2$  illustrating large Stokes shift reported previously.<sup>7</sup>

## References

- 1 J. E. Kroeze, T. J. Savenije, M. J. W. Vermeulen and J. M. Warman, *J. Phys. Chem. B*, 2003, **107**, 7696–7705.
- 2 T. J. Savenije, A. J. Ferguson, N. Kopidakis and G. Rumbles, *J. Phys. Chem. C*, 2013, **117**, 24085–24103.
- 3 H. Oga, A. Saeki, Y. Ogomi, S. Hayase and S. Seki, *J. Am. Chem. Soc.*, 2014, **136**, 13818–13825.
- 4 P. P. Infelta, M. P. de Haas and J. M. Warman, *Radiat. Phys. Chem.* 1977, 1977, **10**, 353–365.
- 5 J. G. Labram, D. H. Fabini, E. E. Perry, A. J. Lehner, H. Wang, A. M. Glaudell, G. Wu, H. Evans, D. Buck, R. Cotta, L. Echegoyen, F. Wudl, R. Seshadri and M. L. Chabiny, *J. Phys. Chem. Lett.*, 2015, **6**, 3565–3571.
- 6 L. M. Herz, *Annu. Rev. Phys. Chem.*, 2016, **67**, 65–89.
- 7 A. R. Pascoe, M. Yang, N. Kopidakis, K. Zhu, M. O. Reese, G. Rumbles, M. Fekete, N. W. Duffy and Y.-B. Cheng, *Nano Energy*, 2016, **22**, 439–452.
- 8 R. Younts, H.-S. Duan, B. Gautam, B. Saparov, J. Liu, C. Mongin, F. N. Castellano, D. B. Mitzi and K. Gundogdu, *Adv. Mater.*, 2016, n/a-n/a.